Electronic Supplementary Material (ESI) for Reaction Chemistry & Engineering.

SUPPORTING INFORMATION

Surface sensitization of g-C_3N_4/TiO_2 via Pd/Rb_2O cocatalysts: Accelerating water splitting reaction for green fuel production in the absence of organic sacrificial agents

KashafUl Sahar[a], KhezinaRafiq[a*], Muhammad Zeeshan Abid[a], Abdul Rauf[a], Ubaid urRehman[b], Ejaz Hussain[a*]

[a]Institute of Chemistry, Inorganic Materials Laboratory 52S, The Islamia University of Bahawalpur-63100, Pakistan

[b] Institute of Physics, Polish Academy of Sciences, Al. Lotników32/46, 02-668 Warsaw, Poland

Corresponding authors email: ejaz.hussain@iub.edu.pk

Section 1

Chemicals required:

All chemicals (analytical grade) used in this work were purchased from commercial sources, and utilized with no additional modification or purification. Melamine was purchased from Hqauiang Chemical Group Stock Co., LTD, andrutile TiO_2 from Texan Minerals & Chemicals. The salt of palladium (II) acetate was purchased from CATO Research Chemicals Incand 99% RbCl (Alfa Aesar, CAS Number 7791-11-9), hydrogen chloride solution (CAS-7647-01-0) and sodium hydroxide (CAS-1310-73-2) from Sigma Aldrich.The high-purity deionized water was facilitated by PIAS Pakistan (PIAS-GW1-Z)

Section 2

Instruments for characterization:

The powder XRD pattern was recorded on anX-ray diffractometer with Ni filtered utilizing Cu-Kα radiation (λ = 1.5418Å, 40 mA, 40kV). Data wascollected by utilizing aflat-plate sample holder in Bragg−Brentano para-focusing geometry. The Fourier transform infrared spectra obtained by KBr tablet in Nicolet avatar 330 FT-IR spectrometer with the unit of cm^{-1}. The chemical composition and morphology were analyzed by SEM images taken by Thermo Fisher AxiaChemiSEM. Diffuse reflectance UV-vis absorption spectra of powdered catalysts obtained from UV-Vis spectrophotometer manufactured by Thermo Fischer Scientific and mounded with the praying mantis diffuse reflectance adapter. X-Ray photoelectron spectroscopy measurements were obtained by using Kratos Axis UlraDLD coupled with a hemispherical deflection analyzer and chamber for analysis. The monochromated Al Kα (1486.6 − 69 eV) was produced by X-rays using a source that put out 150 W and wasutilized for the excitation of the samples (catalysts). For analysis, the samples were carefully pressed into small pellets (0.1 mm width). Raman spectra of the catalysts obtained from Horiba JY LabRAM HR 800 Raman spectrometer joined with amicroscope in reflectance mode (632.8 nm), He-Ne laser (20 mV) with a spectral resolution of 0.35 cm^{-1} and no filter. Additionally, the D4 filter was used to enhance the characteristics of g-C_3N_4, between 1300 − 1800 cm^{-1}. All the catalysts were analyzed at room temperature in the same glass vial to ensure consistent results. The photoluminescence spectroscopy from Custom Cryogenic Macro PL System (CCMPS) coupled with HORIBA components (325 nm laser). The iHR320 was an imaging spectrometer and detection was made by Syncerity CCD.PL is used to examine, whether the as-prepared photocatalysts are appropriate for photocatalytic activity. The electronic structure and band gap of the photocatalysts were obtained from PL. Atomic force microscopywas done by PARK N×10 instrument to determine the mechanical properties and localization of the loaded metals on the surface of photocatalysts. The specified surface area and the diameters of the pores were analyzed by BrunauerEmmmet Teller (BET) technique.

Section 3

Factors affecting the H_2 production activity of photocatalysts

Effect of intensity of light: The water splitting reaction for hydrogen production was performed under sunlight [1, 2]. The hydrogen production efficiency of the photocatalysts is directly proportional to the intensity of light [3]. In the current research, the reactions were performed for 6 hours under solar radiation [4] as shown in Table S1 and Fig S1. The maximum evolution of hydrogen of 19.7 mmol $g^{-1}h^{-1}$was recorded in the 4th hour of reaction from 1:00 PM-2:00 PM.

Table S1. Effect of intensity of light onH_2 evolution by most active photocatalyst in different hours under solar light

Serial No	Photocatalyst	Time under solar light	H_2 Evolution (mmol $g^{-1}h^{-1}$)
1	Pd−Rb_2O@g−C_3N_4/TiO_2	10:00 AM-11.00 AM	6.64
2	Pd−Rb_2O@g−C_3N_4/TiO_2	11:00 AM-12:00 PM	10.3
3	Pd−Rb_2O@g−C_3N_4/TiO_2	12:00 PM-1:00 PM	14.7
4	Pd−Rb_2O@g−C_3N_4/TiO_2	1:00 PM-2:00 PM	19.7
5	Pd−Rb_2O@g−C_3N_4/TiO_2	2:00 PM-3:00 PM	15.4
6	Pd−Rb_2O@g−C_3N_4/TiO_2	3:00 PM-4:00 PM	11.1

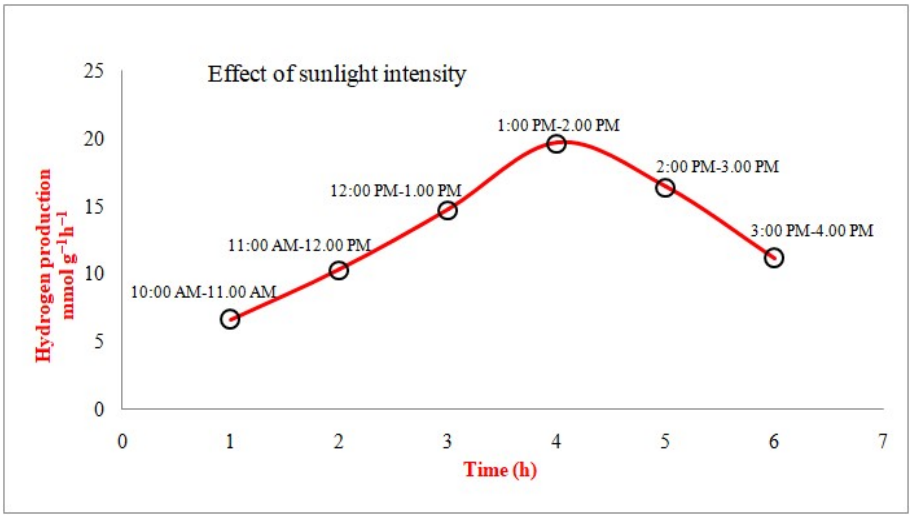

Fig S1: Effect of intensity of light onH_2 evolution by most active photocatalyst in different h under solar light.

Effect of the work function of cocatalysts: The Schottky barrier originates between the metal and semiconductor when the work function of the loaded metal is higher than that of the semiconductor. The work functions of g-C_3N_4 and rutile TiO_2 are 4.62 eV and 4.2 eV as shown in Fig 9 in the main manuscript**.** In current research work, we have found that the high work function of palladium was a key character in efficient H_2 production [5, 6]. The work function of palladium metal is 5.55 eV [7]. To evaluate the difference in hydrogen generation, we have experimented with other metals (metals with low work functions as compared to palladiumi.e.,Cu, Ni, Ru, and Ag) by loading them on the surface of g-C_3N_4/TiO_2. The rate of hydrogen production decreases with the decrease in the work function (Φ) of loaded metals [8] as shown in Table S2 and Fig S2.

Table S2. Effect of the work function of different loaded metals on the support surface (g-C_3N_4/TiO_2) on hydrogen generation (mmol g^{-1})

Metal cocatalyst	**Work function (Φ)**	**Hydrogen production (mmol $g^{-1}h^{-1}$)**
Pd	5.55 eV	19.7
Cu	5.10 eV	17.3
Ni	5.01eV	15.6
Ru	4.71 eV	12.6
Ag	4.26 eV	10.6

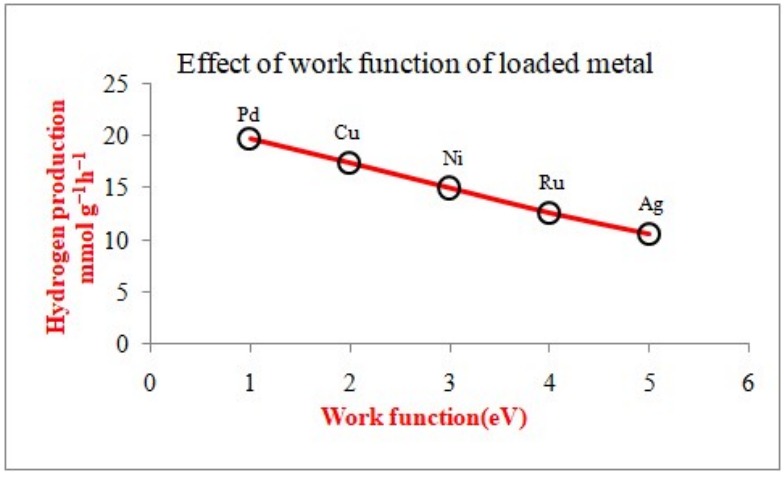

Fig S2: Graphical representation of the effect of work function of different loaded metals on the support surface (g-C_3N_4/TiO_2) on hydrogen generation (mmol g^{-1}).

Effect of pH: The pH is the concentration of H^+ ions present in the solution and the hydrogen production is also affected by the pH [9-11]. Photocatalytic reaction performed at pH 8 where the maximum hydrogen evolution was recorded. While at the high and low pH, the rate of hydrogen evolution reduced, respectively, as shown in Fig S3 and Table S3. The optimized pH analyzed in this current work was pH 8.

Table S3. Effect of pH on hydrogen evolution (mmol $g^{-1}h^{-1}$) by using most active photocatalysts

Photocatalyst	pH	**H_2Evolution (mmol $g^{-1}h^{-1}$)**
Pd−Rb_2O@g−C_3N_4/TiO_2	4.0	4.45
≈ Pd−Rb_2O@g−C_3N_4/TiO_2	5.0	7.98
Pd−Rb_2O@g−C_3N_4/TiO_2	6.0	11.9
Pd−Rb_2O@g−C_3N_4/TiO_2	7.0	15.6
Pd−Rb_2O@g−C_3N_4/TiO_2	8.0	19.7
Pd−Rb_2O@g−C_3N_4/TiO_2	9.0	17.3
Pd−Rb_2O@g−C_3N_4/TiO_2	10.0	14.5

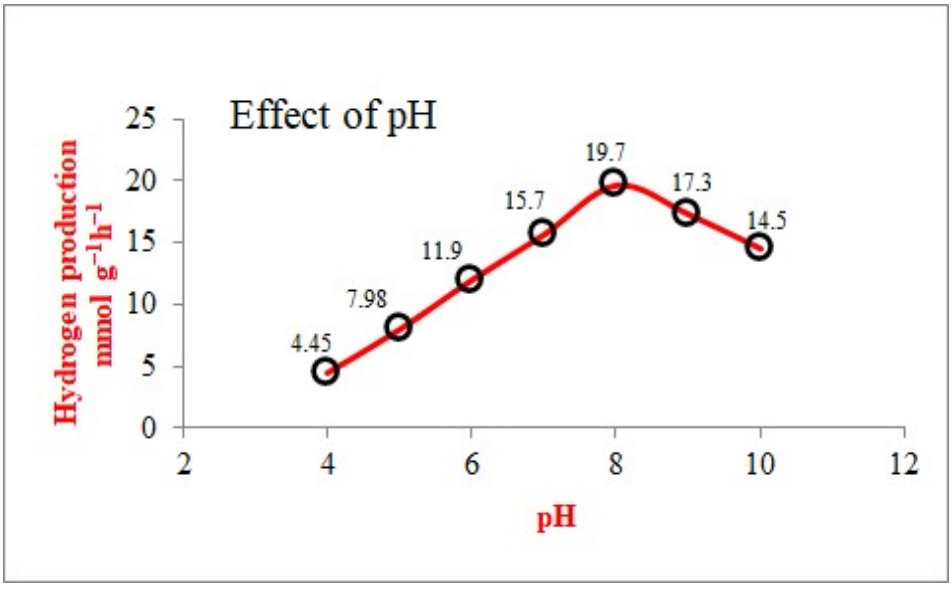

Fig S3: Effect of pH on hydrogen evolution (mmol $g^{-1}h^{-1}$) by using most active photocatalysts

Effect of sacrificial reagent: We have investigated different sacrificial reagents to evaluate their effects on the hydrogen evolution rate [12, 13]. In the current study,the maximum hydrogen

produced is ~19mmol $g^{-1}h^{-1}$ Rb_2O utilized as a cocatalyst as represented in, Table S4 and Fig S4.

Table S4. Effect of nature of sacrificial reagent on hydrogen evolution (mmol $g^{-1}h^{-1}$) by using as-synthesized photocatalysts

Photocatalyst	Sacrificial reagent	H_2 Evolution (mmol $g^{-1}h^{-1}$)
Pd@g−C_3N_4/TiO_2	Glycerol	11.7
Pd@g−C_3N_4/TiO_2	Na_2S	12.8
Pd@g−C_3N_4/TiO_2	S^{2-} /SO_3^2	14.1
Pd@g−C_3N_4/TiO_2	Methanol	16.3
Pd@g−C_3N_4/TiO_2	Ethanol	17.4
Pd−Rb_2O@g−C_3N_4/TiO_2	−	19.7

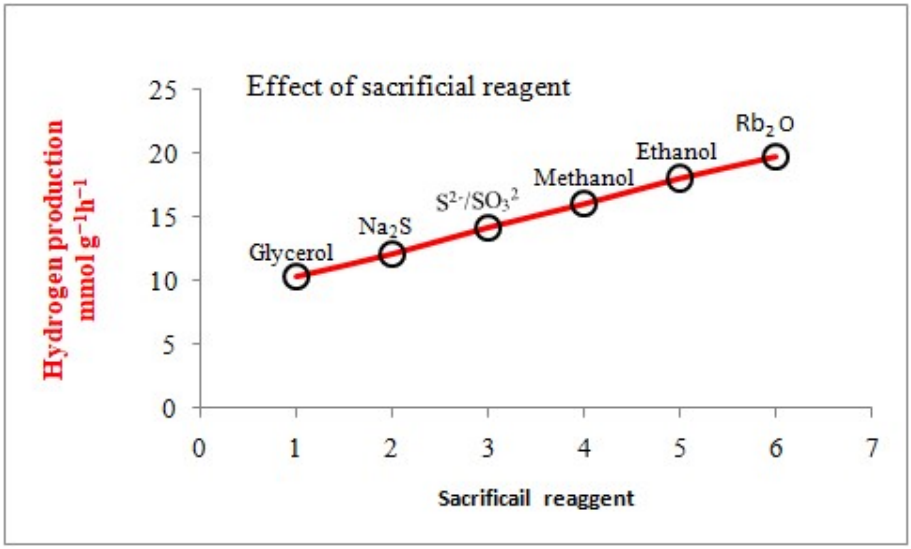

Fig S4: Effect of nature of sacrificial reagent on hydrogen evolution (mmol $g^{-1}h^{-1}$) by using as-synthesized photocatalysts

Effect of dose concentration: We examined the effect dose concentration on the hydrogen production via water splitting reaction [13, 14]. In current research work, of 5 mg was found to be an optimized concentration of photocatalysts which produced 19.7 mmol $g^{-1}h^{-1}$ of hydrogen as represented in Table S5 and Fig S5.

Table S5. Effect of photocatalysts dose on hydrogen evolution (mmol $g^{-1}h^{-1}$) by using as-synthesized photocatalysts

photocatalyst	Concentration	Hydrogen evolution (mmol $g^{-1}h^{-1}$)
Pd−Rb_2O@g−C_3N_4/TiO_2	1 mg	7.69
Pd−Rb_2O@g−C_3N_4/TiO_2	2 mg	10.35
Pd−Rb_2O@g−C_3N_4/TiO_2	3 mg	13.4
Pd−Rb_2O@g−C_3N_4/TiO_2	4 mg	16.5
Pd−Rb_2O@g−C_3N_4/TiO_2	5 mg	19.7
Pd−Rb_2O@g−C_3N_4/TiO_2	6 mg	18.9
Pd−Rb_2O@g−C_3N_4/TiO_2	7 mg	17.6
Pd−Rb_2O@g−C_3N_4/TiO_2	8 mg	15.4

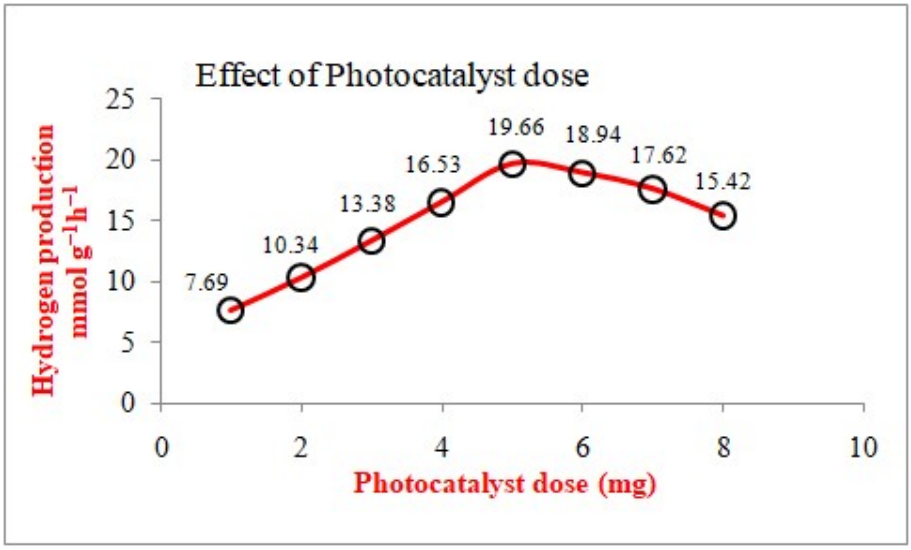

Fig S5: Effect of photocatalysts dose on hydrogen evolution (mmol $g^{-1}h^{-1}$) by using as-synthesized photocatalysts

Section 4

Table S6. Recyclability test for the most active photocatalyst ($Pd-Rb_2O@g-C_3N_4/TiO_2$)

Photocatalyst (**$Pd-Rb_2O@g-C_3N_4/TiO_2$**)	**Time (h)**						**H_2 generation**
	1	2	3	4	5	6	
1st run	13.5	34.6	55.8	76.6	97.3	118.0	mmol g^{-1}
2nd run	12.5	32.6	52.8	72.6	92.3	112.0	mmol g^{-1}
3rd run	11.5	30.6	49.8	68.6	87.3	106.1	mmol g^{-1}

Section 5

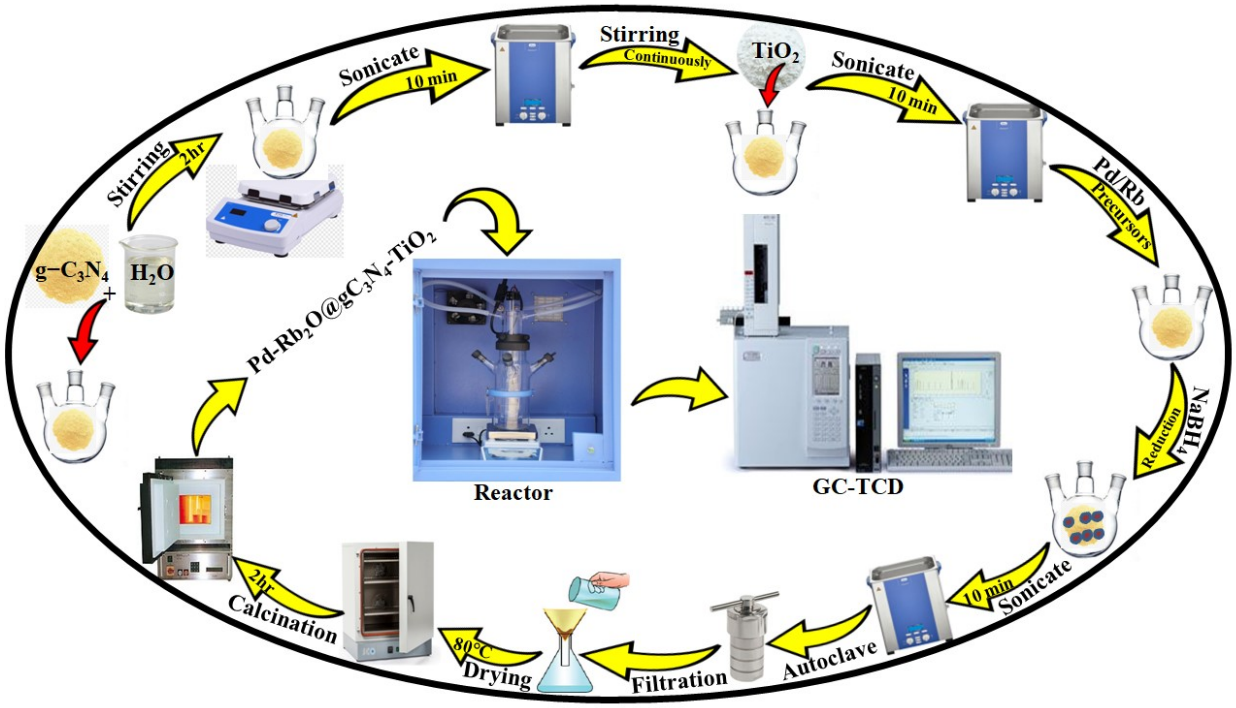

Fig S6: The synthesis scheme of Pd−Rb_2O@g−C_3N_4/TiO_2photocatalysts preparation

Section 6

Table S7. Comparison of quantum efficiency of as-synthesized photocatalysts ($Pd-Rb_2O@g-C_3N_4/TiO_2$) with other metal loaded over TiO_2 semiconductor reported in the literature.

Sr. No	Photocatalyst	Metal loading	Sacrificial reagent	H_2 production (mmol g^{-1} h^{-1})	Quantum yield (%)	Ref.
1.	$Pd-Rb_2O@g-C_3N_4/TiO_2$	1.8:0.2 wt. %	-	19.7	17.7	Present work
2.	Pt/N-TiO_2	1 wt. %	ethanol	2.25	12.3	[15]
3.	Au@TiO_2	0.25 wt.%	methanol	1.25	7.5	[16]
4.	$CuOH_2/TiO_2$	0.29 (mol%)	$C_2H_6O_2$	3.41	13.9	[17]
5.	Au@ TiO_2	0.4 wt. %	methanol	0.36	4.14	[18]
6.	$Ni(OH)_2$/ TiO_2	0.23 (mol%)	methanol	0.3	12.4	[19]
7.	CuO/TiO_2	10 wt. %	ethanol	0.2	5.1	[20]

Section 7

Various %w/w of Pd and Rb_2O over g−C_3N_4/TiO_2: The amount of Pd and Rb_2O, overall, 2 wt% metal was deposited on the surface of the semiconductor(g−C_3N_4/TiO_2).Pd loading was increased (from 0.2 to 1.8 wt. %) at the same time while retaining the overall, metal nanoparticles loading (2 wt. %). It has been observed that thetotal amount of palladium deposited on the surface of the semiconductor(g−C_3N_4/TiO_2)affected the rate of hydrogen production. $Pd_{1.8}$−$Rb_2O_{0.2}$@g−C_3N_4/TiO_2 was found to be the most active photocatalyst in the series. The declining Pd (electron quencher) concentration and increasing Rb_2O concentration up to 1.8 %,ultimately reduced the rate of hydrogen production (GC-TCD experiment). The H_2 generation activities of all photocatalysts including bare TiO_2, g-C_3N_4, g-C_3N_4/TiO_2, $Pd_{0.2}$-$Rb_2O_{1.8}$@g-C_3N_4/TiO_2, $Pd_{0.4}$-$Rb_2O_{1.6}$@g-C_3N_4/TiO_2, $Pd_{0.8}$-$Rb_2O_{1.2}$@g-C_3N_4/TiO_2, $Pd_{1.2}$-$Rb_2O_{0.8}$@g-C_3N_4/TiO_2, $Pd_{1.6}$-$Rb_2O_{0.4}$@g-C_3N_4/TiO_2 and $Pd_{1.8}$−$Rb_2O_{0.2}$@g−C_3N_4/TiO_2 are exhibited in $mmolg^{-1}$ and $mmolg^{-1}h^{-1}$asdemonstrated in Table S8.

Table S8. H_2 generation activities of as-prepared Pd−Rb_2O@g−C_3N_4/TiO_2.

Photocatalysts	**Pd: Rb_2O wt.% ratio**	**H_2 production ($mmol\ g^{-1}$)**	**H_2 production ($mmol\ g^{-1}\ h^{-1}$)**
TiO_2	0	16.4	2.72
g−C_3N_4	0	20.7	3.44
g−C_3N_4/TiO_2	0	64.4	10.7
$Pd_{0.2}$−$Rb_2O_{1.8}$@g−C_3N_4/TiO_2	0.2:1.8	70.2	11.7
$Pd_{0.4}$−$Rb_2O_{1.6}$@g−C_3N_4/TiO_2	0.4:1.6	78.4	13.1
$Pd_{0.8}$−$Rb_2O_{1.2}$@g−C_3N_4/TiO_2	0.8:1.2	81.7	13.6
$Pd_{2.0}$@g−C_3N_4/TiO_2	2 wt. %	90.6	15.1
$Pd_{1.2}$−$Rb_2O_{0.8}$@g−C_3N_4/TiO_2	1.2: 0.8	95.1	15.8
$Pd_{1.6}$−$Rb_2O_{0.4}$@g−C_3N_4/TiO_2	1.6: 0.4	101.4	16.9
$Pd_{1.8}$−$Rb_2O_{0.2}$@g−C_3N_4/TiO_2	1.8: 0.2	118.0	19.7

References:

1. Zhou, P., et al., *Solar-to-hydrogen efficiency of more than 9% in photocatalytic water splitting.* 2023. **613**(7942): p. 66-70.
2. Jawale, N., et al., *Ni loaded SnS 2 hexagonal nanosheets for photocatalytic hydrogen generation via water splitting.* 2023. **13**(4): p. 2418-2426.
3. Ayu, D.G., et al., *Photocatalytic Degradation of Methylene Blue Using N-Doped ZnO/Carbon Dot (N-ZnO/CD) Nanocomposites Derived from Organic Soybean.* 2023.
4. Chong, W.-K., et al., *Non-metal doping induced dual pn charge properties in a single ZnIn2S4 crystal structure provoking charge transfer behaviors and boosting photocatalytic hydrogen generation.* 2023. **325**: p. 122372.
5. Silalahi, R.P.B., et al., *Hydride-containing 2-Electron Pd/Cu Superatoms as Catalysts for Efficient Electrochemical Hydrogen Evolution.* 2023: p. e202301272.
6. Li, L., et al., *Rational design of porous conjugated polymers and roles of residual palladium for photocatalytic hydrogen production.* 2016. **138**(24): p. 7681-7686.
7. Grönbeck, H. and C.J.T.J.o.P.C.C. Barth, *Revealing carbon phenomena at palladium nanoparticles by analyzing the work function.* 2019. **123**(7): p. 4360-4370.
8. Luo, M., et al., *Shape effects of Pt nanoparticles on hydrogen production via Pt/CdS photocatalysts under visible light.* 2015. **3**(26): p. 13884-13891.
9. Ahmed, M.A. and A.A.J.R.a. Mohamed, *Recent progress in semiconductor/graphene photocatalysts: synthesis, photocatalytic applications, and challenges.* 2023. **13**(1): p. 421-439.
10. Paul, D.R., et al., *Mg/Li Co-doped g-C3N4: An excellent photocatalyst for wastewater remediation and hydrogen production applications towards sustainable development.* 2023.
11. Zhang, C. and C.J.R.A. Xue, *Ligand-assisted morphology regulation of AuNi bimetallic nanocrystals for efficient hydrogen evolution.* 2023. **13**(2): p. 1229-1235.
12. Bajpai, H., et al., *Biomass components toward H 2 and value-added products by sunlight-driven photocatalysis with electronically integrated Au δ−−TiO 2: concurrent utilization of electrons and holes.* 2023.
13. Sabir, A.S., et al., *An inclusive review and perspective on Cu-based materials for electrochemical water splitting.* 2023. **13**(8): p. 4963-4993.
14. Hoang, A.T., et al., *Hydrogen Production by Water Splitting with Support of Metal and Carbon-Based Photocatalysts.* 2023.

15. Wu, M.-C., et al., *Nitrogen-doped anatase nanofibers decorated with noble metal nanoparticles for photocatalytic production of hydrogen.* Acs Nano, 2011. **5**(6): p. 5025-5030.
16. Gomes Silva, C.u., et al., *Influence of excitation wavelength (UV or visible light) on the photocatalytic activity of titania containing gold nanoparticles for the generation of hydrogen or oxygen from water.* Journal of the American Chemical Society, 2011. **133**(3): p. 595-602.
17. Yu, J. and J. Ran, *Facile preparation and enhanced photocatalytic H 2-production activity of Cu (OH) 2 cluster modified TiO 2.* Energy & Environmental Science, 2011. **4**(4): p. 1364-1371.
18. Méndez, J.O., et al., *Production of hydrogen by water photo-splitting over commercial and synthesised Au/TiO2 catalysts.* Applied Catalysis B: Environmental, 2014. **147**: p. 439-452.
19. Yu, J., Y. Hai, and B. Cheng, *Enhanced photocatalytic H2-production activity of TiO2 by Ni (OH) 2 cluster modification.* The Journal of Physical Chemistry C, 2011. **115**(11): p. 4953-4958.
20. Yu, Z., et al., *Efficient photocatalytic hydrogen production from water over a CuO and carbon fiber comodified TiO2 nanocomposite photocatalyst.* International journal of hydrogen energy, 2013. **38**(36): p. 16649-16655.